EFFECT OF RIPARIAN VEGETATION ON FLOOD VULNERABILITY: CASE STUDY OF TYPHOON HAGIBIS 2019

Tohoku University, Regular Member, ○Andre Araujo Fortes
Tohoku University, Regular Member, Dr. Masakazu Hashimoto
Tohoku University, Regular Member, Dr. Keiko Udo
Fukken Gijyutsu Consultants Co., Ltd., Regular Member, Ken Ichikawa
Tohoku University, Regular Member, Dr. Shosuke Sato

1 INTRODUCTION

Flood disasters cause great damage to societies. To develop flood control strategies, such as flood vulnerability studies, it is common the use of hydraulic models, tools that depend of many input parameters, such as topographic and hydraulic data and the roughness parameter. The last one is a critical parameter, since it greatly varies according to the surface. The riparian vegetation causes considerable impact in the river flow dynamics, since it is directly related to the roughness parameter. Therefore, the control of the vegetation in the riverbank is important because when in high amount, it can cause the loss of the conveyance capacity, causing embankments. However, in many rivers in Japan, this vegetation management has not been sufficiently carried out. In particular, rivers managed by prefectural governments are rarely managed due to budgetary constraints. Several studies quantified the relationship between the vegetation and the roughness parameter, Wilson (2007) stablished a connection between Manning's coefficient and the degree of submergency of the plants and Devi and Kumar (2016) related the flow resistance with the vegetation density.

UAV photogrammetry is a current trend regarding river mapping of wetland characteristics due to the low cost and low time consumption. Casado et al. (2015) used this approach to identify vegetation.

In October 12, 2019, Tohoku region was hit by Typhoon Hagibis, which caused approximately 140 embankments along more than 70 rivers in Japan, killing 104 people and damaging over 87,000 homes. So, estimation of flood vulnerability is important to the aid in the prevention and mitigation of such damage.

The objective of this study is to quantitatively estimate the effect of riparian vegetation on flood vulnerability using the real severe case of Typhoon Hagibis in 2019.

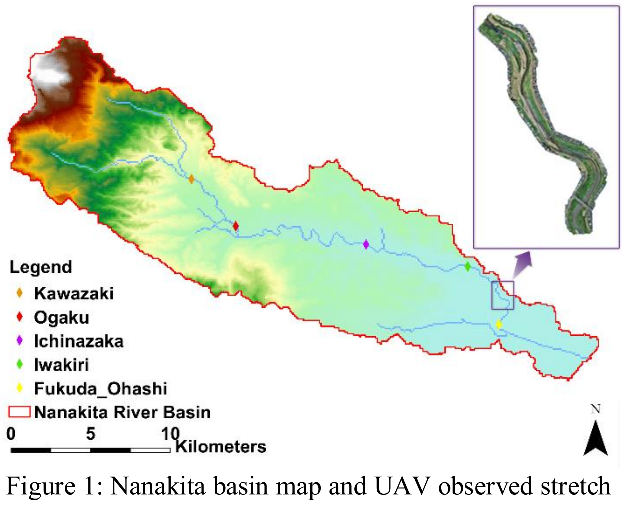

Figure 1: Nanakita basin map and UAV observed stretch

2 METHODOLOGY

The study area of this research is the Nanakita river. A class-B river located in Miyagi prefecture, passing by the cities of Sendai and Tagajo, with 40.9 km of length and 229.1 km² of catchment area. This river was selected since class-B are small rivers, where the vegetation varies more yearly and its effect is more perceptible. Figure 1 shows the map of river catchment. For this research, a 2.23 km stretch of the river, shown in Figure 1, was selected for the flood vulnerability study with the 2D hydraulic simulation. This stretch was chosen because it is well vegetated and, although the water level was high, overtopping have not occurred during typhoon Hagibis, therefore the scenario is ideal to perform flood vulnerability analysis by assessing the amount of vegetation.

The methodology was divided in 2 phases. Phase 1 is the hydrologic model and phase 2 is the 2D hydraulic model. The hydrological simulation was performed with RRI model, a 2D model that performs rainfall-runoff-inundation simulations (see (Sayama et. Al. (2012)).

The input data used in the model was: (1) observed rainfall data collected from 7 rainfall gauge stations with hourly observation of 48 hours from October 12 to 13 of 2019, (2) MERIT Hydro DEM with 90 m was used for the topographic data (see (Yamazaki et al., 2019)), (3) land cover map from the Ministry of Land, Infrastructure, Transport and Tourism, created in 2014 with 100 m resolution and (4) cross sections provided from Miyagi prefecture for the five gauge stations shown in Figure 1.

For this model, it was adopted a Manning of 0.03 for the river channel. In the slope area, the Manning values were 0.2 for vegetated areas, 0.4 for urban areas and 0.03 for water bodies. The discharge calculated from a H-Q formula for Iwakiri gauge station was used to validate the simulation.

After the completion of phase 1, the hydraulic simulation was performed. The input parameters of this model are the topographic data, the upstream discharge and the roughness. The outputs are the water elevation map and the water level profile. For this phase, the topographic data

Keywords UAV-SfM, Manning's Roughness, Flood Vulnerability, Typhoon Hagibis
Contact Information 〒980-8572 Aoba 468-1, Aramaki, Aoba-ku, Sendai, Japan, Phone number: 022-752-2114

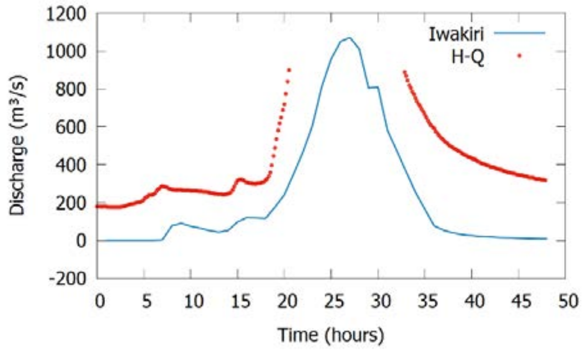

Figure 2: Comparison between simulated and observed discharge at Iwakiri gauge station

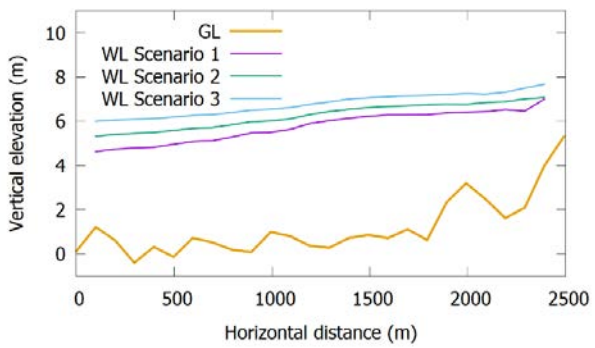

Figure 3: Comparison of water level profiles between scenarios 1, 2 and 3

was constructed by interpolating the 100 m spaced cross sections provided by Miyagi prefecture, creating a 2D mesh with 10 m resolution. The use of 10 m grid cell was chosen to reduce the computation time cost. The hydraulic data used for input was the discharge obtained from phase 1 in the upstream part of the UAV observed stretch. Three scenarios were simulated, (1) with a single Manning of 0.022, (2) with Manning 0.022 and 0.038 for river channel and overbank areas respectively, to simulate the riparian vegetation outside the channel, and (3) with Manning 0.038 for the entire topography, assuming both the channel and overbank areas with vegetation.

3 RESULTS AND DISCUSSION

In phase 1 it could be noted that the simulation showed results close to observed. In Iwakiri station the hydrograph shows a peak discharge around 1070 m^3/s by the 27^{th} hour from the start of the simulation. Regarding the validation of the simulation, the hydrograph in Iwakiri was compared with the discharges calculated from the H-Q formula.

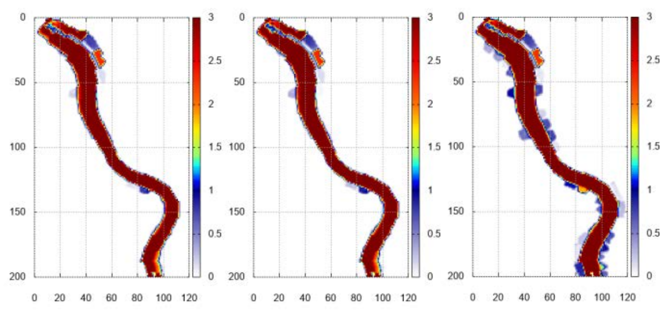

Figure 4: Comparison of flood mark between scenarios 1 (left), 2 (center) and 3(right)

Figure 2 shows the comparison between observed and simulated discharges at Iwakiri station. It can be observed that the rise of discharge from the simulation occurs later when compared to the observed. This might have occurred due to the lack of initial conditions in the model.

In phase 2, the simulated inundations reached different water level profiles. Scenario 1 presented the lowest water level and scenario 3, the highest. The water level profiles for the 3 scenarios in the peak hour (27^{th}) can be seen in Figure 3. It can be observed that, as vegetation increases, the conveyance capacity of the channel is compromised, provoking the increase in the water level. Figure 4 shows the inundation map comparison of scenario 1, 2 and 3.

Analyzing the flood extent of the 3 scenarios it can be seen the interaction between the roughness and the conveyance capacity. In scenario 1 there is only one flood spot beyond the levee structures. Scenario 2 showed 8.78% of average increase in the water level of the area relative to scenario 1, showing a similar overtopping. Scenario 3 presented 18.01% of average increase relative to scenario 1. Figure 4 presents several locations where overtopping of the levees has occurred in scenario 3. The overtopping that occurred in these scenarios happened also due to an underestimation of the levee's heights due to the cross sections' interpolation process for the 2D mesh construction.

4 CONCLUSION

Variations in the vegetation caused considerable changes in the water level at the peak discharge. The results showed an average increase in the water level of 8.78% from scenario 1 to 2 and 18.01% from scenario 1 to 3. In addition, the consideration of the vegetation effect in scenarios 1, 2 and 3 have shown the flood vulnerability of the observed area, presenting overtopping in scenario 3, where the vegetation was considered more abundant. In this case, average water level was used, but in further studies, precise evaluation can be done with the use of high-resolution imagery from UAV observations.

5 REFERENCES

Casado, M.R., Gonzalez, R.B., Kriechbaumer, T., and Veal, A., 2015. Automated identification of river hydromorphological features using UAV high resolution aerial imagery. *Sensors*, 15, 27969–27989.

Devi, T.B., and Kumar, B., 2016. Experimentation on submerged flow over flexible vegetation patches with downward seepage. *Ecol. Eng*, 91, 158–168.

Sayama, T., Ozawa, G., Kawakami, T., Nabesaka, S. and Fukami, K., 2012. Rainfall–runoff–inundation analysis of the 2010 Pakistan flood in the Kabul River basin. *Hydrological Sciences Journal*, 57, 298-312.

Wilson, C.A.M.E., 2007. Flow resistance models for flexible submerged vegetation. *J Hydrol (Amst)*, 342, 213–222.

Yamazaki, D., Ikeshima, D., Sosa, J., Bates, P.D., Allen, G., and Pavelsky, T., 2019. MERIT Hydro: A high-resolution global hydrography map based on latest topography datasets. *Water Resour. Res.*, 55, 5053-5073.